Microstructural Characterization of Additively Manufactured Ti-6Al-4V With the Addition of β-Stabilizer, Niobium

Khutso Mrwata[1*], *Charles* Siyasiya[1], and *Nana* Arthur[2]

[1] University of Pretoria, Department of Materials Science and Metallurgical Engineering, South Africa
[2]CSIR, Photonics Centre, Laser Enabled Manufacturing, Pretoria Campus, South Africa

Abstract. This study investigated the influence of beta stabilizer niobium on the microstructure and hardness of Ti-6Al-4V. The relationship between increased the concentration of alloying elements into Ti-6Al-4V is generally associated with an increase in hardness due to solid solution strengthening. The research involved the fabrication of a series of laser engineering net shaping (LENS™) Ti-6Al-4V alloys with varying concentrations of niobium (13%, 20%, and 28%) to determine whether increasing the Nb content has an influence on the concentration of Nb dissolved into Ti-6Al-4V. The microstructures of these alloys were analysed the hardness examined. the results revealed that the solid solution strengthening did not lead to a proportional increase in hardness as expected. Further microstructural examination showed that the alloy with 13% Nb exhibited a distinct microstructure with a higher concentration of un-melted Nb particles, whereas the alloy with 28% Nb had a higher dissolution of Nb into the Ti-6Al-4V. The least percentage of Nb dissolved into the Ti-6Al-4V compared to the addition of 28% Nb. Increased Nb content resulted in a higher percentage of Nb dissolved in Ti-6Al-4V but the lower hardness value. The undissolved Nb did not contribute solid solution strengthening but rather the presence of defects, and features of microstructure are responsible for hindering the ease of plastic deformation.

1 Introduction

In recent years the application of additive manufacturing (AM) for medical applications has been embraced by the medical industry especially in the orthopaedic surgery department where implants have been being fabricated using AM [1]. Among those implants includes spinal rods, spinal fusion rods or spinal instrumentation, which are medical devices used in orthopaedic surgery to stabilize and support the spine [2]. They are commonly employed in procedures such as spinal fusion, correction of spinal deformities (e.g., scoliosis), and treatment of spinal fractures [3].

* Khutso Mrwata : u11031906@tuks.co.za

The use of AM has presented many adventitious reasons for fabricating spinal rods; the function of these rods is dependent on application, and selection of the rods are dependent on the patient's condition, the level of spinal involvement, and the surgical approach chosen by the healthcare professionals [4]. The following advantages make AM a preferable choice for manufacturing spinal rods: its ability to create highly complex geometries and customized designs where spinal rods can be produced with intricate internal structures, and/or patient-specific features that allow for spinal rods to be lightweight without compromising the material's strength or durability but significantly reducing the overall weight burden on the patient's spine [4]. Additionally, AM allows for rapid prototyping and iterative design improvements, thus, producing a rapid development timeline which is vital for patient cases where time is a critical factor, such as patient-specific implants or emergency surgeries [2]. LENS™ is a type of AM technique that utilizes a high-power laser to selectively melt and fuse metallic powder particles layer by layer, enabling precise and customizable fabrication of complex metal components. Its application in biomedical implant production offers the potential to create patient-specific, biocompatible implants with tailored geometries, fostering improved implant integration and patient outcomes [2, 12].

Despite these advantages, there are limitations associated with the application of laser engineering net shaping LENS™ spinal rods. The first limitation is the lack of long-term studies that assess the longevity and effectiveness of LENS™ spinal rods which is required to definitively make claims about their efficiency and safety over long periods [3]. In terms of the materials used for the production of LENS™ spinal rods, there are lack of comparative studies with the conventionally manufactured spinal rods [4]. This has made it difficult for direct comparisons to be made for clinical outcomes and complications compared to traditional spinal rods, thus, limited assessment of the advantages and disadvantages associated with their application [3].

Considering the above-mentioned limitations, this study aims to contribute to the ongoing research into β-alloys manufactured using direct energy deposition (DED), LENS™, AM to allow for comparative evaluations to be done regarding the materials that may be appropriate for application for LENS™ spinal rods. In addition, to determine whether increasing the Nb content will have an influence on the concentration of Nb dissolved into Ti-6Al-4V. This study will further allow for assessment of the benefits, limitations, and patient selection for Ti-6Al-4V with Nb addition LENS™ spinal rod implant application.

The hypothesis of this study is that an increase in the Nb content in Ti-6Al-4V alloy manufactured using LENS™ will result in an increase in hardness. This hypothesis is based on the assertion that solid solution strengthening increases with the addition of beta stabilizers in Ti-6Al-4V and thus increases the hardness value of Ti-6Al-4V [6].

The premise of the hypothesis was to vary the amounts of Nb content (13, 20 and 28%) added to LENS™ Ti-6Al-4V and study the corresponding changes associated with the microstructures using microstructural analysis techniques such as scanning electron microscopy (SEM), energy-dispersive x-ray spectroscopy (EDS) and optical microscopy (OM. Also, to see the effect of increasing Nb content on the hardness of the alloy. The hardness measurements were conducted using the Vickers hardness tester. The investigation involves a comparative analysis of hardness values among the samples and a subsequent discussion regarding the influence of microstructural variations in each alloy on these values. Throughout this study, a consistent set of processing conditions and alloy composition for Ti-6Al-4V is maintained. To acquire a more comprehensive understanding of the effect of Nb on the hardness of LENS™ manufactured Ti-6Al-4V, an isolated evaluation of hardness is conducted, independently of other mechanical properties.

2 Literature Review

2.1 Additive Manufacturing

Additive manufacturing, also known as 3D printing, is a process of creating three-dimensional objects by adding successive layers of material [7]. It is a revolutionary manufacturing technique that allows complex geometries and customized designs to be produced with high precision [9]. Instead of traditional subtractive methods that involve cutting or shaping a material to obtain the desired shape, additive manufacturing builds objects layer by layer from the ground up [9].

Direct Energy Deposition (DED) is a specific additive manufacturing technique that involves the use of a focused energy source, such as a laser or electron beam, to melt and fuse materials together [7]. In DED, a feedstock material, often in the form of a powder or wire, is deposited onto a substrate, and the energy source is precisely controlled to melt the material and create a solid object [9]. This technique is particularly suitable for fabricating large, complex, and high-value parts [9].

Laser Engineering Net Shaping (LENS^{TM}) is a specific type of DED process that utilizes a high-power laser to melt and fuse metal powders, creating fully dense, near-net shape components [9]. LENS^{TM} technology enables the production of complex metal parts with excellent material properties [4]. The process involves the precise deposition of powdered metal onto a substrate while simultaneously melting it with a laser beam [9]. LENS^{TM} can be used for prototyping, repair, and refurbishment of existing components, or even the creation of fully functional end-use parts [10].

2.2 Beta alloys in orthopaedic surgery

Beta alloys, also known as beta titanium alloys, are a type of metallic alloy that contains a significant amount of the beta-phase titanium crystal structure [6]. These alloys are primarily composed of titanium along with other elements such as aluminium, vanadium, and molybdenum [5]. The presence of beta-phase crystals gives these alloys their distinctive properties, including high strength, excellent corrosion resistance, and good biocompatibility [11].

Beta alloys are being used in spinal rods (medical implants used in spinal fusion surgeries to provide stability and support to the spine while it heals [3].) due to their desirable characteristics [12]. Beta alloys offer several advantages for spinal rod applications including: a high strength-to-weight ratio, exhibit a unique combination of strength and flexibility, making them suitable for spinal rod applications, excellent corrosion resistance, which is important for implants that remain in the body for an extended period, good biocompatibility, meaning they are well-tolerated by the human body and have a low risk of triggering immune responses or complications [2, 15]. Overall, the use of beta alloys in spinal rods allows the production of durable, lightweight, and biocompatible implants that provide stability and support during the healing process after spinal fusion surgery.

3 Methodology

Three samples of Ti-6Al-4V with added Nb (13%, 20% and 28%), % volume fraction, concentrations were created in-situ using the LENS™ system with a 1 kW IPG fibre laser and a co-axial powder delivery nozzle at 360 W power at a speed of 8.4 m/s onto a Grade 5 titanium alloy plates of 5 mm thickness. The plates were cleaned via sandblasting and wiped with acetone. The materials used for deposition, Ti-6Al-4V (ELI) and Nb were powdered

and with particle sizes between of 40 – 100 µm, were deposited at varying flow rates and rpm values.

The samples were then cut laterally to reveal the interior surface. Metallographic preparation was conducted followed by etching with Kroll's solution to reveal the microstructure. Optical microscopy and microstructural techniques, SEM and EDS were conducted using JEOL JSM-6510.

A Matsuzawa Vickers micro-hardness tester, at a load of 300 g for a dwell time of 10 s for each indentation, was used to conduct the hardness testing on each sample. The indentations placed on the prepared surface of the samples at a spacing of 500 µm between the indentations, there were 15 indents placed on each sample.

4 Results

The microstructure of Ti-6Al-4V, Figure 1, manufactured using LENS^{TM}, has the Widmanstätten pattern and columnar prior beta grains visible from the optical microscopic. The microstructure associated with LENS^{TM} produced Ti-6Al-4V contains the Widmanstätten pattern and α-laths throughout the microstructure [11]. The microstructure of Ti-6Al-4V appears as the Widmanstätten pattern which consists of interleaved bands or plates with different crystal orientations. The formation of this pattern is a result of the transformation from the high temperature the β-phase to the lower temperature α-phase [12]. These α-phase plates form as lath-like structures known as α-laths or α-lamellae within the beta matrix in specific crystallographic orientations [13]. The α-laths, in Ti-6Al-4V play a crucial role in determining the mechanical properties of the alloy. The arrangement, size, and distribution of the α-laths can influence the alloy's mechanical properties. They contribute to the strength and hardness of the material [13].

The grain morphology consists of columnar grains that grow towards the heat flow direction during slower cooling rates or directional solidification [12]. These grains tend to have a dendritic or column-like structure [13]. Figure 1 contains these prior β-phase grains associated with planar solidification in AM Ti-6Al-4V.

Refining the microstructure of Ti-6Al-4V is done with either heat treatments or the addition of alloying elements which often result in a uniform distribution of α-laths and improved mechanical properties [13]. The addition of niobium refines the microstructure of Ti-6Al-4V by inhibiting the growth of columnar grains [12]. The Nb altered the solidification mechanism, from planar solidification to cellular solidification Ti-6Al-4V. This is evident in microstructures that contain Nb, Figures 2 (a), (b), and (c) where the grains have been altered from columnar grains to equiaxed grains.

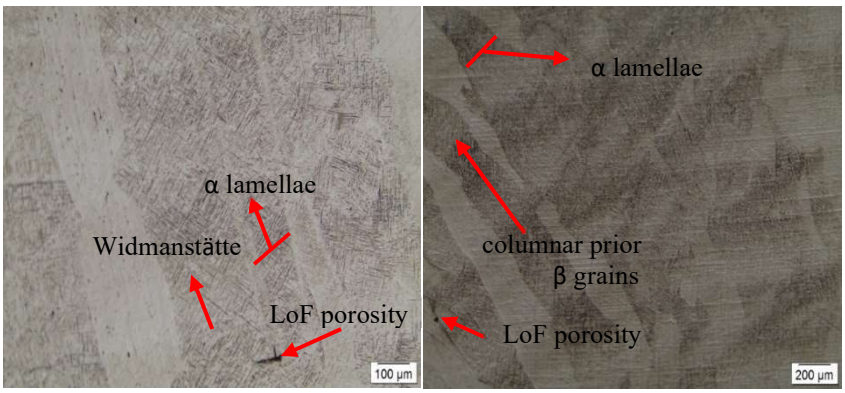

Fig. 1. Optical microscope images of the microstructure of Ti-6Al-4V manufacture using LENS^{TM}.

Alloy Ti-6Al-4V-13Nb consists of dark coloured α-laths that are thin, and needle shaped arranged in mismatched orientations. At the bottom of the sample, Figure 2 (a), the Widmanstätten pattern is present along with gas porosity. Further along the sample, in the middle of the sample, there is an increase in both the density and size of lack of fusion (LoF) porosity. In Figure 3 (a), the Widmanstätten pattern is no longer visible but rather longer α-laths appear scattered throughout the microstructure. The density of un-melted Nb particles increased in the built direction. At the top of the sample, Figure 4 (a), the microstructure appears like the microstructure in Figure 3 (a) except there is an increase in the presence of α-laths and the un-melted Nb particles have increased in size.

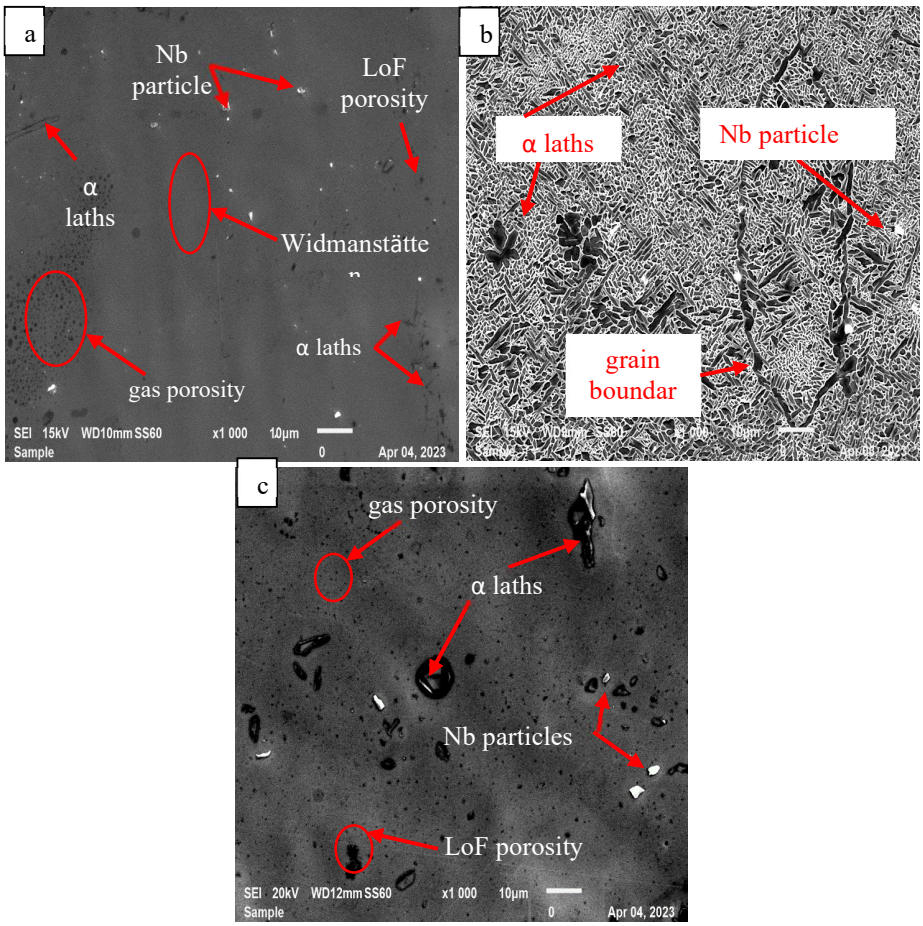

Fig. 2. Microstructure of (a) Ti-6Al-4V-13Nb, (b) Ti-6Al-4V-20Nb, and (c) and Ti-6Al-4V-28Nb.

Figure 2 (b), Ti-6Al-4V-20Nb, consists of a microstructure with multiple variants of thicker and thinner Widmanstätten α-laths. The larger α-laths lie within the grains, along the grain boundary or cut across them, while others have agglomerated together. Furthermore, Figure 2 (b) contains the intersection of three grain boundaries with the dark semi-spherical and white dots of un-melted particles. The microstructure also consists of the Widmanstätten basketweave pattern. Like the microstructure of Ti-6Al-4V-13Nb, the microstructure of Ti-6Al-4V-20Nb also has an increase in the presence of un-melted Nb compared to Ti-6Al-4V. The α-laths in Figure 3 (b) are shorter, almost spherical, and more uniform compared to the α-laths in Figure 2 (b). The α-laths in the microstructure at the top of the sample Ti-6Al-4V-

20Nb, Figure 4 (b), consists of shorter and thicker α-laths obtained within the grains and along the grain boundaries, while the larger α-laths have further increased in size and agglomerated together, and are located within and across grains, and along the grain boundary boundaries.

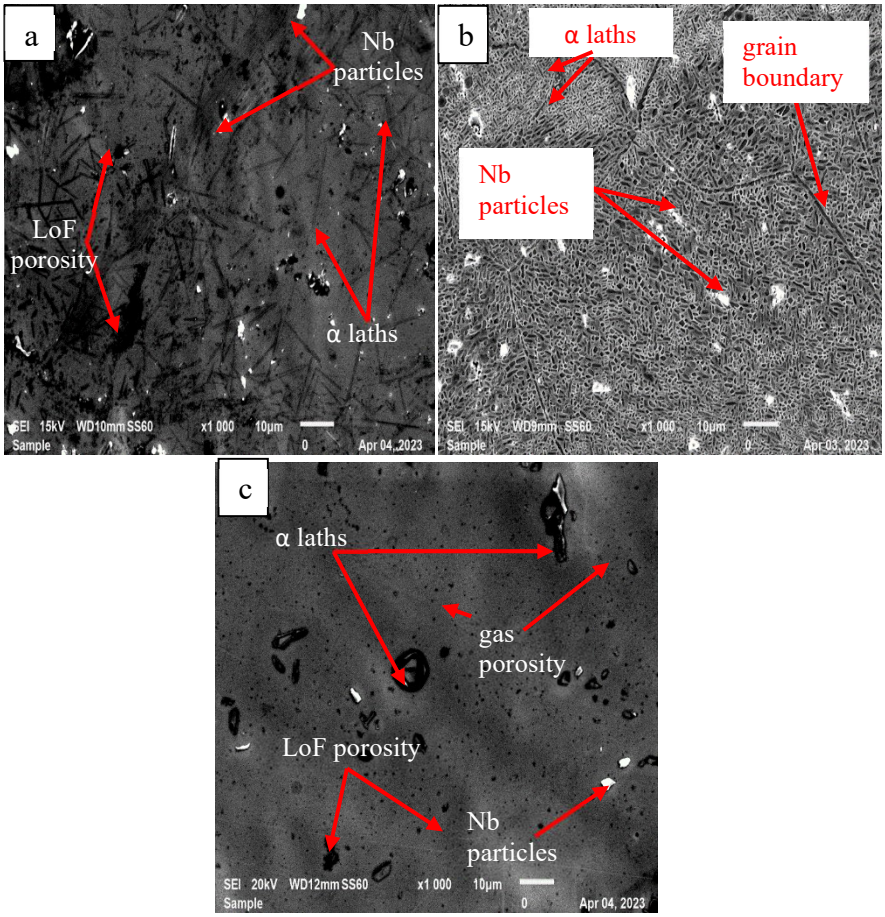

Fig. 3. Microstructure of Ti-6Al-4V-13Nb (a), Ti-6Al-4V-20Nb (b), and Ti-6Al-4V-28Nb (c), middle of sample.

Finally, the microstructure of alloy Ti-6Al-4V-28Nb, Figure 2 (c) consists of the lowest density of α-laths compared to the other alloys. The α-laths have formed thicker laths that have agglomerated together to form larger α-laths. Figure 3 (c), the middle of sample Ti-6Al-4V-28Nb, has increased presence of α-laths that are thinner and longer than those observed in Figure 2 (c). The top of the sample has a similar microstructure to Figure 3 (c) with shorter α-laths. Unlike the other alloys, the density of un-melted Nb appears to lowest in the microstructure of Ti-6Al-4V-28Nb while porosity is more predominate in this alloy. The colour of the microstructure is affected by phases present in each sample. In terms of contrast, all Figures 2, 3, and 4 have a greyish colour with varying amounts of black. The lighter phase between the dark α-laths, which appear as darker/black, is the β-phase while the semi-spherical white dots distributed within the microstructure are the un-melted Nb particles. Comparing the contrast between Figures 2 (a), 3 (a), and 4 (a), it appears that reduced presence of the dark laths may correlate to the increase in the β-phase which appears lighter and increase in Nb content.

The shift from planar to cellular solidification is generally accompanied by the segregation of the alloying elements added to Ti-6Al-4V [12], Figures 2, 3, and 4 all have un-melted Nb particles with the presences of these particles increasing as the Nb %vol fraction increases. The grains in Figure 5 appear roughly spherical or cuboidal in shape. The microstructures of the alloys vary from each other and within themselves. All the Nb containing alloys have the following similar microstructural features and defects present, firstly the microstructural similarities are the presence of α-laths, and secondly the following defects, lack of fusion (LoF) porosity and, un-melted Nb particles.

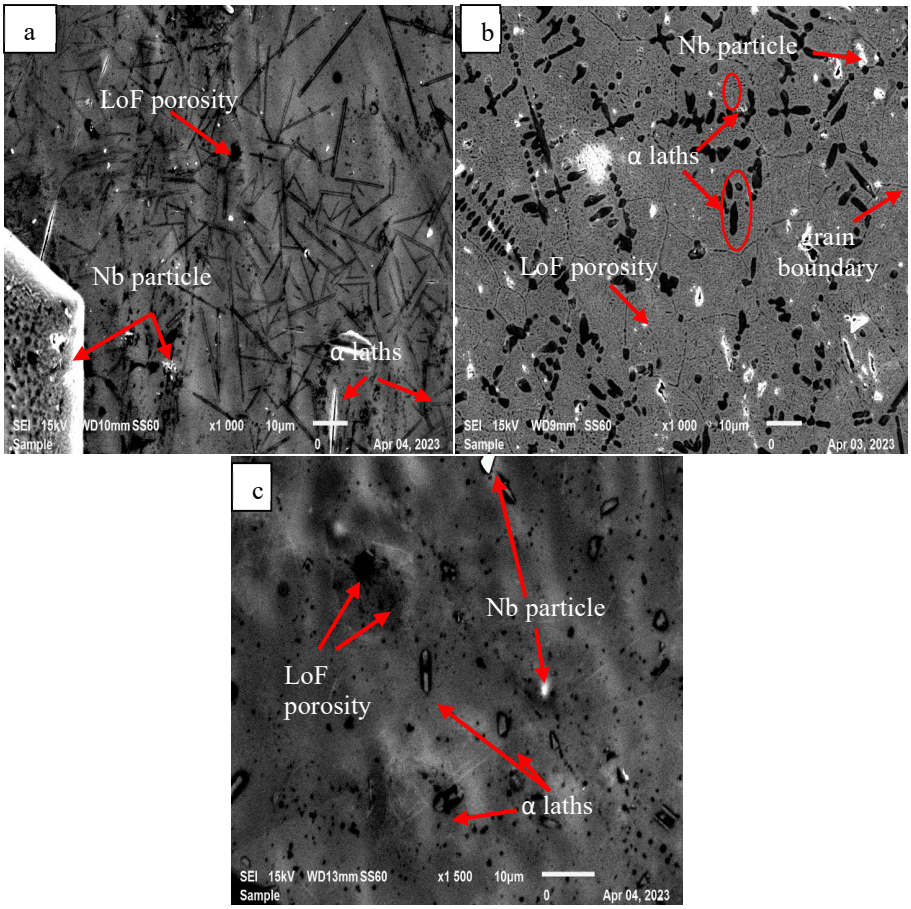

Fig. 4. Microstructure of Ti-6Al-4V-13Nb (a), Ti-6Al-4V-20Nb (b), and Ti-6Al-4V-28Nb (c), located at the top of sample.

Table 1. Hardness values for each alloy.

Alloy	**Ti-6Al-4V**	**Ti-6Al-4V-13Nb**	**Ti-6Al-4V-20Nb**	**Ti-6Al-4V-28Nb**
Hardness (HVN)	343	333	302	208
Deviation (%)	-	3	12	40
%Vol Nb dissolved	-	12.7	20.3	28.5

Nb addition to Ti-6Al-4V results in an overall decrease in hardness, Figure 6, with the effect pronounced with the addition of 28% Nb where there is 40% difference between the hardness values of Ti-6Al-4V and Ti-6Al-4V-28Nb, summarized in Table 1. Figure 7 illustrates the %vol fraction Nb distribution throughout the sample, where the position on the sample is indicated by T-top, M-middle, B-bottom, L-left, R-right, C-centre, i.e., TC is top centre of the sample. Ti-6Al-4V-13Nb had the least variation throughout the sample while Ti-6Al-4V-28Nb has the most variation. From the Figure 6 and 7, it may be presumed that the increasing the Nb content in Ti-6Al-4V results in decreased hardness values because of the increased %vol fraction of Nb that is undissolved in Ti-6Al-4V, thus, not contributing to solid solution strengthening. The values in Table 1 were obtained from EDS analysis. Multiple points across the surface of each sample were analysed and from the results of the analysis, which included a concentration of each element at each point, an average was calculated for the Nb.

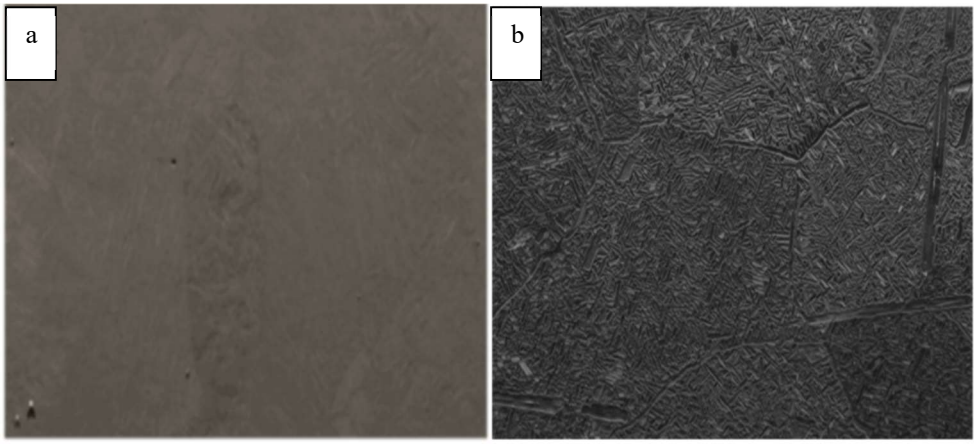

Fig. 6. Columnar grains in Ti-6Al-4V, a, and equiaxed grains Ti-6Al-4V-20Nb, b.

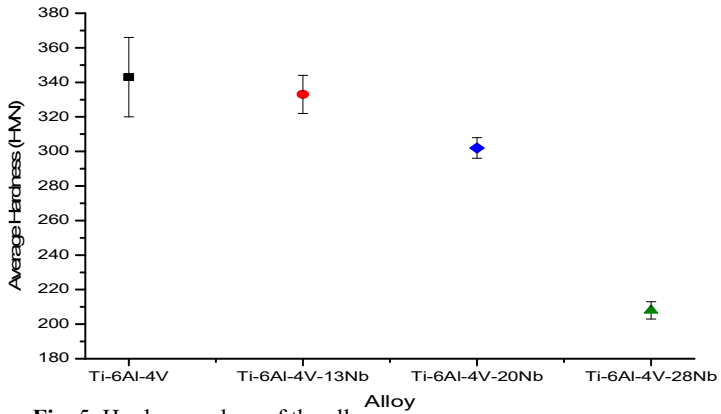

Fig. 5. Hardness values of the alloys.

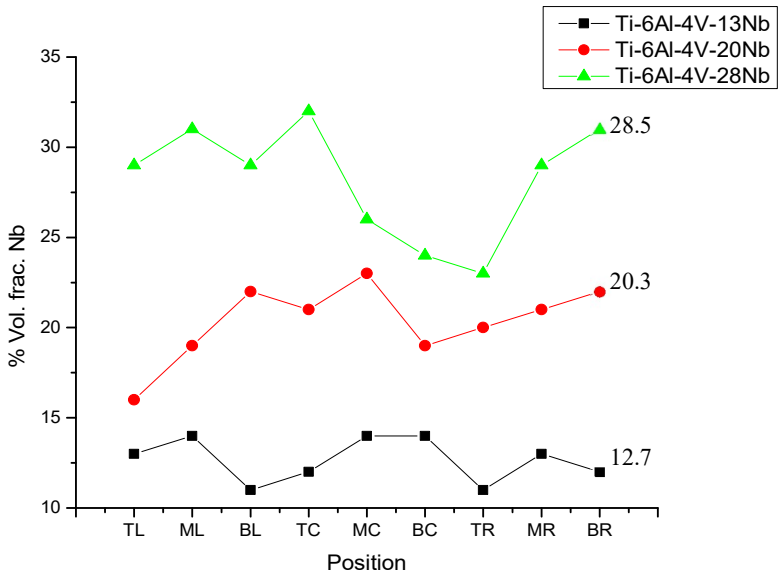

Fig. 7. Distribution of %vol Nb fraction throughout the sample and the average %vol Nb fraction for the sample.

5 Discussion

The results indicate that the microstructure of Ti-6Al-4V was altered by the addition of Nb and that these changes impacted the hardness values. Figure 1 is the typical microstructure associated with LENS^{TM} produced Ti-6Al-4AV. The notable differences between Figure 2 and Figures 3, 4, and 5 are the size, orientation, and distribution of the α-laths, and porosity. As the size of the α-laths increased, their orientation become more randomized while their distribution and density varied, Figures 3, 4 and 5.

Although hardness may be correlated to the α-laths size, the relationship between lath size and hardness is not linear and can depend on various factors [12]. For instance, alloy Ti-6Al-4V-28Nb consists of thicker laths but exhibited the lowest hardness value while the alloy Ti-6Al-4V-13Nb with the thinner laths exhibited the higher hardness value. This may be due to the decreased density of α-laths observed in Ti-6Al-4V. The decrease in laths removes the barriers to dislocation movement, which hinders plastic deformation and consequently, decreased the hardness of the alloy.

The grains in alloy Ti-6Al-4V changed from columnar to equiaxed with the addition of Nb. These grains are referred to as equiaxed because they have similar dimensions in all directions [13]. Their formation is a result of either certain processing conditions, rapid solidification, and or the addition of alloying elements [2].

Alloy Ti-6Al-4V-28Nb consists of thicker α-laths with low density and increased visible porosity. This alloy exhibited the lowest hardness value, 208 HVN despite having larger α-laths, which have larger cross-sectional areas and normally increase the density of barriers which impedes the plastic deformation of the material and increase the hardness but the reduced density of α-laths in this alloy overrides the impact of the thickness on hardness. The increase in porosity creates voids where localized stress concentrations increase allowing for deformation to occur, thus, reducing hardness values. Moreover, lower hardness values are associated with the β-phase and the decrease in α-laths in Ti-6Al-4V-28Nb may correlated to a decrease in the alpha phase present in the alloy [12].

The equiaxed grains are accompanied by high density of grain boundaries where dislocations can traverse through them which reduces the resistance to plastic deformation, thus lowering the hardness [13]. These grains have random distribution of crystallographic orientations which results in a lower volume fraction of grains aligned in specific preferred orientations since preferred crystallographic orientations are associated with increased resistance to dislocation movement which increases values [13].

The suggested hypothesis states that introducing and further addition of niobium into the Ti-6Al-4V will correlate to an increase in hardness values due to solid solution strengthening. However, this is encumbered on the amount of Nb that dissolves and contributes to solid solution strengthening. Figure 7 illustrates the variation of Nb %vol fraction throughout the alloys, with Ti-6Al-4V-13Nb having the least variation and highest hardness value. While alloy Ti-6Al-4V-28Nb exhibited the most variation in %Nb concentration and the lowest hardness value. This increase in %vol Nb variation may suggest that as the Nb content increases, less of it contributes to solid solution strengthening, therefore a decrease in hardness. Contrary to the hypothesis, the hardness values decreased in relation to increasing Nb addition to Ti-6Al-4V. This decrease in overall hardness of LENS^{TM} Ti-6Al-4V may be attributed to microstructural changes, reduced presence of the α-laths, i.e., alpha phase, increased defects, porosity density, un-melted Nb particles, and Nb that did not contribute to solid solution strengthening.

Hardness values are important to consider for spinal rods; however, they are not a critical factor nor the sole determinant of the implant's success. This is because hardness is a measure of a material's resistance to localized deformation using indentation limited to the surface of the material while strength measurements represent the material's ability to withstand applied loads without permanent deformation or failure for the bulk of the material [13]. Thus, spinal rod implants are not expected to exhibit high hardness measurements as the primary requirement for their functionality and effectiveness. This means that the decreased hardness value obtained for Ti-6Al-4V-28Nb would suffice for the application of spinal rods since the focus of the mechanical properties and characteristics of spinal rod implants are evaluated and tailored for the specific needs of each patient and this value range lies for hardness values for this application.

6 Conclusion

In light of the results presented, the notion that increasing the %vol fraction of Nb to Ti-6Al-4V will result to higher hardness values is no longer tenable. Microstructural properties, grain morphology, porosity and defects, their distribution, indirectly impact the hardness, thus, challenging the hypothesis that suggests solid solution strengthening increases with increasing Nb %vol fraction which, subsequently, increases the hardness.

The claim made in the hypothesis relies on the assumption that the %vol fraction Nb added to Ti-6Al-4V contributes to solid solution strengthening. From the results, alloy Ti-6Al-4V-13Nb exhibited the highest hardness and lowest variation in the %vol fraction Nb found throughout the sample compared to Ti-6Al-4V-28Nb which exhibited the opposite behaviour. This may be attributed to the pronounced density of un-melted Nb particles and α-laths compared to alloy Ti-6Al-4V-13Nb that exhibited the least variation in %vol Nb fraction throughout the sample along with decreased α-lath density of and increased porosity.

This suggests that the changes in the microstructure override solid solution strengthening, since it appears that more Nb dissolved into both Ti-6Al-4V-13Nb and Ti-6Al-4V-28Nb with the latter exhibiting the lowest hardness value.

Further research is necessary to investigation and explore the impact of Nb on the complex interplay between hardness and phase transformation from alpha to beta, beta phase

retained, and grain refinement and coarsening. This understanding may allow for improved material selection and design for spinal rod implants.

References

1. B. Wang, *The Effect of 3D Printing Metal Materials on Osteoporosis Treatment.* Biomed Res Int, **2021**: 9972867 (2021)
2. S. Ohrt-Nissen, *Sagittal Alignment After Surgical Treatment of Adolescent Idiopathic Scoliosis*, Application of the Roussouly Classification. Spine Deformity **6**(5): 537-544 (2018)
3. A. Warburton, *Biomaterials in Spinal Implants: A Review.* Neurospine **17**(1): 101-110 (2020).
4. Y. Marsumi, and A. W. Pramono, *Influence of Niobium or Molybdenum in Titanium Alloy for Permanent Implant Application.* Advanced Materials Research **900**: 53-63 (2014).
5. R. Banerjee, *Microstructural evolution in laser deposited compositionally graded a/b titanium-vanadium alloys.* Acta Materialia **51**: 3277–3292. (2003)
6. S. A. M. Tofail, *Additive manufacturing: scientific and technological challenges, market uptake and opportunities.* Materials Today **21**(1): 22-37. (2018)
7. D. Svetlizky, *Directed energy deposition (DED) additive manufacturing: physical characteristics, defects, challenges and applications.* Materials Today **49**: 271-295. (2021).
8. M. R. Maina *Laser Additive Manufacturing of Titanium-Based Implants.* Advanced Manufacturing Techniques Using Laser Material Processing**:** 236-247. (2016)
9. G. Gong, *Research status of laser additive manufacturing for metal: a review.* Journal of Materials Research and Technology, **15**: 855-884. (2021)
10. S. S.Sidhu, *A review on alloy design, biological response, and strengthening of beta-titanium alloys as biomaterials.* Mater Sci Eng C Mater Biol Appl **121**: 111661 (2021).
11. S. Bose, *Additive manufacturing of biomaterials.* Prog Mater Sci **93**: 45-111 (2018).
12. M. Sarraf, *A state-of-the-art review of the fabrication and characteristics of titanium and its alloys for biomedical applications*. Bio-Design and Manufacturing, **5**: 371–395 (2022).
13. J. D. Cotton, *State of the Art in Beta Titanium Alloys for Airframe Applications.* JOM **67**(6): 1281-1303 (2015).
14. S. B. Gabriela, *The Effect of Niobium Content on the Hardness and Elastic Modulus of Heat-Treated Ti-10Mo-Xnb Alloys.* Materials Research **13**(3): 333-337. (2010).
15. N. K. K. Arthur, *Microstructural Response of Ti6Al4V ELI Alloyed with Molybdenum by Direct Energy Deposition.* Journal of Materials Engineering and Performance **30**(7): 5455-5465. (2021).
16. G. Lutjering, *Microstructure and Mechanical Properties of Titanium Alloys.* (Unknown).
17. I. Damisih, N. Jujur, J, Sah, D.H. Prajitno, *Characteristics microstructure and microhardness of cast Ti-6Al-4V ELI for biomedical application submitted to solution treatment.* (2018).

18. M. Peters, C. Leyens and M. Peters, *Titanium and Titanium Alloys Fundamentals and Applications.* Cologne, Germany, WILEY-VCH Verlag GmbH & Co. KGaA, Weinheim**:** 1-35. (2003).
19. M. J. Jackson, *Titanium and Titanium Alloy Applications in Medicine.* Surgical Tools and Medical Devices**:** 475-517. (2016).